PCCP

Physical Chemistry Chemical Physics

This paper is published as part of a PCCP Themed Issue on:

Interfacial Systems Chemistry: Out of the Vacuum, Through the Liquid, Into the Cell

Guest Editors: Professor Armin Gölzhäuser (Bielefeld) & Professor Christof Wöll (Karlsruhe)

Self-assembled monolayers of benzylmercaptan and *para*-cyanobenzylmercaptan on gold: surface infrared spectroscopic characterization
K. Rajalingam, L. Hallmann, T. Strunskus, A. Bashir, C. Wöll and F. Tuczek, *Phys. Chem. Chem. Phys.*, 2010
DOI: 10.1039/b923628g

The formation of nitrogen-containing functional groups on carbon nanotube surfaces: a quantitative XPS and TPD study
Shankhamala Kundu, Wei Xia, Wilma Busser, Michael Becker, Diedrich A. Schmidt, Martina Havenith and Martin Muhler, *Phys. Chem. Chem. Phys.*, 2010
DOI: 10.1039/b923651a

Geometric and electronic structure of Pd/4-aminothiophenol/Au(111) metal–molecule–metal contacts: a periodic DFT study
Jan Kučera and Axel Groß, *Phys. Chem. Chem. Phys.*, 2010
DOI: 10.1039/b923700c

Ultrathin conductive carbon nanomembranes as support films for structural analysis of biological specimens
Daniel Rhinow, Janet Vonck, Michael Schranz, Andre Beyer, Armin Gölzhäuser and Norbert Hampp, *Phys. Chem. Chem. Phys.*, 2010
DOI: 10.1039/b923756a

Microstructured poly(2-oxazoline) bottle-brush brushes on nanocrystalline diamond
Naima A. Hutter, Andreas Reitinger, Ning Zhang, Marin Steenackers, Oliver A. Williams, Jose A. Garrido and Rainer Jordan, *Phys. Chem. Chem. Phys.*, 2010
DOI: 10.1039/b923789p

Model non-equilibrium molecular dynamics simulations of heat transfer from a hot gold surface to an alkylthiolate self-assembled monolayer
Yue Zhang, George L. Barnes, Tianying Yan and William L. Hase, *Phys. Chem. Chem. Phys.*, 2010
DOI: 10.1039/b923858c

Holey nanosheets by patterning with UV/ozone
Christoph T. Nottbohm, Sebastian Wiegmann, André Beyer and Armin Gölzhäuser, *Phys. Chem. Chem. Phys.*, 2010
DOI: 10.1039/b923863h

Tuning the local frictional and electrostatic responses of nanostructured $SrTiO_3$—surfaces by self-assembled molecular monolayers
Markos Paradinas, Luis Garzón, Florencio Sánchez, Romain Bachelet, David B. Amabilino, Josep Fontcuberta and Carmen Ocal, *Phys. Chem. Chem. Phys.*, 2010
DOI: 10.1039/b924227a

Influence of OH groups on charge transport across organic–organic interfaces: a systematic approach employing an "ideal" device
Zhi-Hong Wang, Daniel Käfer, Asif Bashir, Jan Götzen, Alexander Birkner, Gregor Witte and Christof Wöll, *Phys. Chem. Chem. Phys.*, 2010
DOI: 10.1039/b924230a

A combinatorial approach toward fabrication of surface-adsorbed metal nanoparticles for investigation of an enzyme reaction
H. Takei and T. Yamaguchi, *Phys. Chem. Chem. Phys.*, 2010
DOI: 10.1039/b924233n

Structural characterization of self-assembled monolayers of pyridine-terminated thiolates on gold
Jinxuan Liu, Björn Schüpbach, Asif Bashir, Osama Shekhah, Alexei Nefedov, Martin Kind, Andreas Terfort and Christof Wöll, *Phys. Chem. Chem. Phys.*, 2010
DOI: 10.1039/b924246p

Quantification of the adhesion strength of fibroblast cells on ethylene glycol terminated self-assembled monolayers by a microfluidic shear force assay
Christof Christophis, Michael Grunze and Axel Rosenhahn, *Phys. Chem. Chem. Phys.*, 2010
DOI: 10.1039/b924304f

Lipid coated mesoporous silica nanoparticles as photosensitive drug carriers
Yang Yang, Weixing Song, Anhe Wang, Pengli Zhu, Jinbo Fei and Junbai Li, *Phys. Chem. Chem. Phys.*, 2010
DOI: 10.1039/b924370d

On the electronic and geometrical structure of the *trans*- and *cis*-isomer of tetra-*tert*-butyl-azobenzene on Au(111)
Roland Schmidt, Sebastian Hagen, Daniel Brete, Robert Carley, Cornelius Gahl, Jadranka Dokić, Peter Saalfrank, Stefan Hecht, Petra Tegeder and Martin Weinelt, *Phys. Chem. Chem. Phys.*, 2010
DOI: 10.1039/b924409c

Oriented growth of the functionalized metal–organic framework CAU-1 on –OH- and –COOH-terminated self-assembled monolayers
Florian Hinterholzinger, Camilla Scherb, Tim Ahnfeldt, Norbert Stock and Thomas Bein, *Phys. Chem. Chem. Phys.*, 2010
DOI: 10.1039/b924657f

Interfacial coordination interactions studied on cobalt octaethylporphyrin and cobalt tetraphenylporphyrin monolayers on Au(111)
Yun Bai, Michael Sekita, Martin Schmid, Thomas Bischof, Hans-Peter Steinrück and J. Michael Gottfried, *Phys. Chem. Chem. Phys.*, 2010
DOI: 10.1039/b924974p

Probing adsorption and aggregation of insulin at a poly(acrylic acid) brush
Florian Evers, Christian Reichhart, Roland Steitz, Metin Tolan and Claus Czeslik, *Phys. Chem. Chem. Phys.*, 2010
DOI: 10.1039/b925134k

Nanocomposite microstructures with tunable mechanical and chemical properties
Sameh Tawfick, Xiaopei Deng, A. John Hart and Joerg Lahann, *Phys. Chem. Chem. Phys.*, 2010
DOI: 10.1039/c000304m

Microstructured poly(2-oxazoline) bottle-brush brushes on nanocrystalline diamond

Naima A. Hutter,[a] Andreas Reitinger,[b] Ning Zhang,[a] Marin Steenackers,[a] Oliver A. Williams,[c] Jose A. Garrido*[b] and Rainer Jordan*[ad]

Received 11th November 2009, Accepted 20th January 2010
First published as an Advance Article on the web 18th February 2010
DOI: 10.1039/b923789p

We report on the preparation of microstructured poly(2-oxazoline) bottle-brush brushes (BBBs) on nanocrystalline diamond (NCD). Structuring of NCD was performed by photolithography and plasma treatment to result in a patterned NCD surface with oxidized and hydrogenated areas. Self-initiated photografting and photopolymerization (SIPGP) of 2-isopropenyl-2-oxazoline (IPOx) resulted in selective grafting of poly(2-isopropenyl-2-oxazoline) (PIPOx) polymer brushes only at the oxidized NCD areas. Structured PIPOx brushes were converted by methyl triflate into the polyelectrolyte brush macroinitiator for the living cationic ring-opening polymerization (LCROP) of 2-oxazolines. The LCROP was performed with 2-ethyl-2-oxazoline (EtOx) as well as 2-(carbazolyl)ethyl-2-oxazoline (CarbOx) as monomers, resulting in structured bottle-brush brushes (BBB) with different pendant side chains and functionalities. FT-IR spectroscopy, fluorescence microscopy, and AFM measurements indicated a high side chain grafting density as well as quantitative and selective reactions. Poly(2-oxazoline) BBBs containing hole conducting carbazole moieties on NCD as electrode material may open the way to advanced amperometric biosensing systems.

Introduction

Doped diamond substrates, including single-, poly-, nanocrystalline (NCD) and ultrananocrystalline diamond (UNCD), have gained tremendous interest as electrode materials due to their unique properties. The large electrochemical potential window, chemical inertness, physicochemical stability, and biocompatibility make diamond especially suitable for amperometric biosensing applications.[1–4] Recent developments in diamond growth by chemical vapor deposition (CVD), give access to large-area synthetic diamond surfaces at reasonable costs. However, the defined chemical functionalization of diamond surfaces as mediating layers between the electrode material and biological systems is still a subject of intense research. Two different approaches have been developed for the controlled attachment of organic molecules to H-terminated diamond. We reported on the spontaneous grafting of aromatic diazonium salts on hydrogenated UNCD resulting in densely packed and homogeneous self-assembled monolayers[5] while Hamers *et al.*[6,7] reported on the photochemical functionalization of polycrystalline diamond surfaces with terminal alkenes. Using the second approach, some of us demonstrated that proteins can be covalently immobilized on NCD surfaces without losing their biological functionality.[8,9]

In contrast to SAMs that allow defined but only monolayer functionalization, the surface coupling of redox active moieties, biomolecules or recognition sites *via* polymer brushes bearing multiple functions on a single grafted chain are very promising. They allow the design of biosensors with significant higher loading capacities per unit area and thus, potentially enhanced sensitivity. Even densely grafted polymer chains that extend from the surface into the adjacent liquid phase are accessible by large organic molecules. Due to the flexibility of the grafted chains, the liquid phase penetrates the polymer layer and molecules can interact with binding partners deep within the layer. Compared to the direct immobilization of molecules on flat surfaces, this three dimensional arrangement of binding sites allows a modular design modeling of biomimetic systems.[10] Furthermore, the soft polymer interface typically stabilizes biomolecules better than two dimensional self-assembled monolayers (SAMs) and proteins can maintain their native conformation, selectivity and enzymatic activity.[11–15]

The preparation of polymer brushes on diamond surfaces has been the subject of only a few studies.[16–18] Existing approaches are based on the pre-modification of the diamond substrate with an organic monolayer, followed by surface-initiated polymerization. Recently, we have shown that polystyrene (PS) brushes could be prepared directly on OH-terminated diamond by the self-initiated photografting and photopolymerization (SIPGP) of styrene.[19] The SIPGP process is a straightforward synthetic route to obtain dense

[a] *Wacker-Lehrstuhl für Makromolekulare Chemie, Department Chemie, TU München, Lichtenbergstraße 4, 85747 Garching, Germany. E-mail: Rainer.Jordan@tu-dresden.de*
[b] *Walter Schottky Institut, TU München, Am Coulombwall 3, 85748 Garching, Germany. E-mail: Jose.Garrido@wsi.tum.de*
[c] *Fraunhofer Institute for Applied Solid State Physics, Tullastraße 72, 79108 Freiburg, Germany*
[d] *Professur für Makromolekulare Chemie, Department Chemie, TU Dresden, Zellescher Weg 19, 01069 Dresden, Germany*

and well defined polymer brush layers without the introduction of specific surface-bonded initiators.[20,21] However, glassy hydrophobic PS brushes are not suitable for the immobilization of biomolecules. Instead, more hydrophilic, biocompatible and multifunctional polymers are desirable. Up to now, poly(ethylene glycol) (PEG) has been the most widely used polymer,[22–25] but current PEG systems have major limitations for long-term applications. It has been reported that PEG coatings lose their function when placed *in vivo* and can undergo oxidative degradation.[4,26,27] Poly(2-oxazoline)s (POx) have recently come into focus as a potential alternative to the well established PEG systems.[28–32] It has been shown that POx is non-toxic and that proteins as well as drugs can be coupled to the polymer without losing their activity.[28–29,31,33] POx show a great variability due to possible terminal as well as pendant functionalization.[34–39] We recently reported on the preparation of homogeneous and very stable poly(2-isopropenyl-2-oxazoline) (PIPOx) brushes on polished glassy carbon by the SIPGP of 2-isopropenyl-2-oxazoline (IPOx).[40] The pendant oxazoline ring of the PIPOx brushes was used to perform a consecutive living cationic ring-opening polymerization (LCROP) with different 2-alkyl-2-oxazoline monomers resulting in so-called bottle-brush brushes (BBBs). Such bottle-brush structures show striking resemblance to the molecular architecture of various polyglycans located on nearly every living cell[41,42] and are regarded as biomimetic moieties that may have high potential for tailoring the interface between semiconductors and biological systems. Based on our recent work on the preparation of BBBs on glassy carbon, we here report on the synthesis of structured poly(2-oxazoline) BBBs on nanocrystalline diamond surfaces. As the grafting reaction is similar, we now take advantage of the reactivity difference between hydrogenated and oxidized diamond for a selective SIPGP[19] which allows an area specific grafting and thus results in microstructured polymer brushes on patterned H-/OH-terminated NCD samples. The consecutive LCROP forming the polymer brush pendant chains was performed with 2-ethyl-2-oxazoline (EtOx) as well as 2-(carbazolyl)-ethyl-2-oxazoline (CarbOx) as the monomers. The interest of the functionalization of BBs with pendant carbazole units in the side chain is twofold. First, polymers containing carbazole side chains are of special interest, as they are known to be electrically conductive. Such polymers are hole transporting materials by a hopping mechanism involving adjacent carbazole units.[43,44] For the fabrication of electrically conductive, hydrophilic, and biocompatible polymer brushes on diamond for amperometric biosensors, poly(2-oxazoline) BBBs with carbazole moieties constitute an intriguing system. Secondly, the fluorescence of the carbazole unit offers a direct way to determine if a sterically demanding oxazoline monomer (CarbOx) can be introduced effectively into a BBBs by means of surface-initiated living cationic polymerization using grafted macroinitiators.

The combination of the unique properties of NCD as electrode material and the biocompatibility as well as variability of the poly(2-oxazoline) layer may open the way to stable biosensing systems with enhanced biocompatibility.

Experimental section

Materials

Chemicals were purchased from Sigma-Aldrich (Steinheim, Germany) or Acros (Geel, Belgium) and used as received unless otherwise stated. Methyl triflate (MeOTf), 2-ethyl-2-oxazoline (EtOx) and acetonitrile (ACN) were dried by refluxing over CaH_2 under a dry argon atmosphere and were freshly distilled prior to use.

Nanocrystalline diamond (NCD)

NCD was grown by microwave plasma enhanced chemical vapor deposition. Prior to growth, prime grade 100 silicon wafers were cleaned with standard SC1 solution and seeded with a colloid of monodisperse diamond nanoparticles known to realize nucleation densities in excess of 10^{11} cm^{-2}.[57] The growth conditions were 3% CH_4 diluted in hydrogen at a pressure of 50 mbar. The microwave power was 3500 W and the film was grown to 150 nm thickness in around 25 min; the temperature was 700 °C.

Clean NCD surfaces were hydrogenated in a commercial microwave plasma reactor (AX5010) using a hydrogen flow 100 sccm, hydrogen pressure 50 mbar and microwave power of 750 W during 15 min. The structuring was performed using a Shipley S1818 photoresist that was spin-coated at 6000 rpm with a MicroTec MJB 3 mask aligner (Süss, Garching, Germany). After exposure (Mercury i-line) and development, the samples were oxidized in a Technics Plasma 100-E plasma system (oxygen pressure 1.4 mbar, microwave power 200 W, 5 min). The photoresist was removed by ultrasonication in acetone and 2-propanol.

2-Isopropenyl-2-oxazoline (IPOx)

IPOx was synthesized according to Seeliger *et al.*[36]

2-(Carbazolyl)ethyl-2-oxazoline (CarbOx)

CarbOx was synthesized following a route described by Hsieh and Litt.[45] Bromopropionitrile was added dropwise to a suspension of carbazole (1 eq.) and *tert*-butylammoniumbromide (0.03 eq.) in NaOH (50%) and benzene at room temperature (RT). After 2 h, the reaction was quenched with hot water. The resulting yellow precipitate was filtered and washed with hot water. After recrystallization in ethanol, the obtained *N*-propionitrile-carbazol was dissolved in aminoethanol (1.4 eq.) and *n*-butanol. Cadmium acetate dihydrate (0.03 eq.) was added and the reaction mixture stirred under reflux for 24 h at 140 °C. After evaporation of the solvent the residue was purified by recrystallization in hexane to give CarbOx as a colorless solid.

^{1}H NMR: δ ppm 8.10 (m, 2H), 7.45 (m, 4H), 7.24 (m, 2H), 4.65 (m, 2H), 4.18 (t, J = 9.43 Hz, 2H), 3.80 (t, J = 9.63 Hz, 2H), 2.81 (m, 2H); 13C NMR: δ ppm 27.32, 39.70, 54.41, 67.36, 108.45, 119.10, 120.42, 123.01, 125.71, 139.95, 165.68; IR (KBr): 3047 (m), 2952 (m), 1669 (s).

Self-initiated photopolymerization and photografting (SIPGP)

Freshly prepared and structured NCD substrates were submerged in approximately 2 mL of distilled and degassed

IPOx in a photoreaction tube under dry argon atmosphere. Polymerization was allowed to complete within 20 h under constant irradiation with UV light (300–400 nm; λ_{max} = 350 nm) at RT. After SIPGP, the samples were immediately cleaned by sequential ultrasonication with ethanol, ACN, ethyl acetate (all HPLC grade) for 5 minutes each.

Living cationic ring-opening polymerization (LCROP)

The poly(2-isopropenyl-2-oxazoline) (PIPOx) modified NCD substrates were submerged in a solution of 2 mL dry and freshly distilled acetonitrile (ACN) with an excess amount of methyl trifluoromethane sulfonate (MeOTf) at approximately −35 °C under a dry argon atmosphere. After stirring for 3 h at 0 °C, the mixture was allowed to equilibrate to RT and stirred for 60 min before EtOx or CarbOx was added under argon atmosphere. In the case of the side chain LCROP with CarbOx, 2 mL of dry ACN were added at this point. The reaction solution was stirred at 80 °C for 16 h. Finally, an excess of piperidine was added to selectively terminate the LCROP. After 60 min, the sample was removed from the reaction solution and thoroughly washed with a saturated solution of potassium carbonate in deionized water (Millipore). Final cleaning was performed by sequential ultrasonication in deionized water, ethanol, ACN and ethyl acetate for 5 min each.

Infrared spectroscopy (FT-IR)

Infrared spectroscopy (FT-IR) was performed on an IFS 55 Bruker instrument equipped with a diffuse reflectance Fourier transform infrared (DRIFT) setup from SpectraTech and a mercury–cadmium–telluride (MCT) detector. For each spectrum, 500 scans were accumulated with a spectral resolution of 4 cm^{-1}. Background spectra were recorded on freshly prepared hydrogenated NCD samples.

Atomic force microscopy (AFM)

AFM scans were obtained with a Nanoscope IIIa scanning probe microscope from Veeco Instruments using standard tips in tapping mode (driving amplitude of ~1.25 V at a scan rate of 0.5 Hz). The average roughness (rms) was calculated from a representative 2 μm^2 large area.

Fluorescence microscopy

Fluorescence microscopy images were obtained with a Leica DMI 6000 B microscope equipped with a Hamamatsu C4742 camera. The sample was irradiated using a Leica Fluo A filter cube (BP340-380 nm). The cross-section analysis was performed by pixel analysis of the 256 bit black and white fluorescence image using the public domain *Image J* software package.

^{1}H- and ^{13}C nuclear magnetic resonance (NMR)

NMR spectra were recorded on a Bruker ARX 300 (1H, 300.13 MHz and 13C, 75.48 MHz) with tetramethylsilane as internal standard at T = 293 K in $CDCl_3$.

Results and discussion

The preparation of microstructured bottle-brush brushes (BBBs) on nanocrystalline diamond (NCD) is outlined in Fig. 1. First, a hydrogenated NCD substrate was patterned by conventional photolithography. The exposed areas were oxidized in an oxygen plasma. After removal of the photoresist and thorough cleaning, the partially oxidized NCD substrate was submerged in bulk 2-isopropenyl-2-oxazoline (IPOx) and irradiated under UV light (λ_{max} = 350 nm) for 20 h for the self-initiated photografting and photopolymerization (SIPGP).[40]

After SIPGP, the substrate was again thoroughly cleaned by ultrasonication in acetonitrile, ethyl acetate, and ethanol for 5 minutes each to remove only physisorbed material. AFM measurements revealed that a dense and homogeneous polymer brush layer with a thickness of 79 ± 8 nm was selectively formed on the oxidized NCD areas (Fig. 2). Data analysis of the AFM scans gave a surface roughness on polymer coated regions with an rms of 5.4 nm, which is significantly lower as compared to the bare NCD surface regions (rms 9.6 nm). The change of the layer surface morphology shows the formation of a homogeneous and continuous brush that completely screens the oxidized NCD substrate. The reactivity contrast between the H- and OH-terminated surface areas during the SIPGP process is in agreement with our recent account on the SIPGP of styrene on ultrananocrystalline diamond (UNCD).[19] In the SIPGP mechanism, the monomer acts as a photosensitizer, activating a surface functional group by hydrogen abstraction to start a free radical surface-initiated polymerization.[21] The selective formation of polymer brushes on the OH-terminated areas can be explained by the difference in bond dissociation energy (BDE) of C–H (401.5 kJ mol^{-1})[46] and O–H bonds (71 kJ mol^{-1})[19] on diamond. The measured brush height is in good agreement with our recently reported kinetic studies on the SIPGP of IPOx on polished glassy carbon substrates.[40]

The formation of PIPOx brushes was confirmed by FT-IR measurements (Fig. 3). The strong bands at 1650 cm^{-1} (amide I) and 1193 cm^{-1} can be assigned to the stretching vibration modes of C=N and C–O in the 2-oxazoline ring.[40]

The monomer 2-isopropenyl-2-oxazoline (IPOx) has two orthogonal polymerizable groups, namely the vinyl group used for the SIPGP and the 2-oxazoline ring for the living cationic ring-opening polymerization (LCROP). Very recently, we have used this dual-functionality of IPOx to prepare defined bottle brushes by the polymerization of IPOx by living anionic or free radical polymerization with consecutive LCROP[47] as well as brushes of bottle brushes on polished glassy carbon (GC).[40] First, the PIPOx brushes were converted into a polycationic macroinitiator followed by the side chain cationic polymerization of 2-substituted-2-oxazolines. Here, an analogous approach was employed for the preparation of micro-structured P(IPOx-*g*-EtOx) and P(IPOx-*g*-CarbOx) BBBs on NCD.

The conversion of the neutral PIPOx brushes into the cationic polyelectrolyte was achieved by submerging the modified NCD substrate in a solution of methyl triflate in acetonitrile for 5 h. The P($IPOx^+OTf^-$) brush layer was

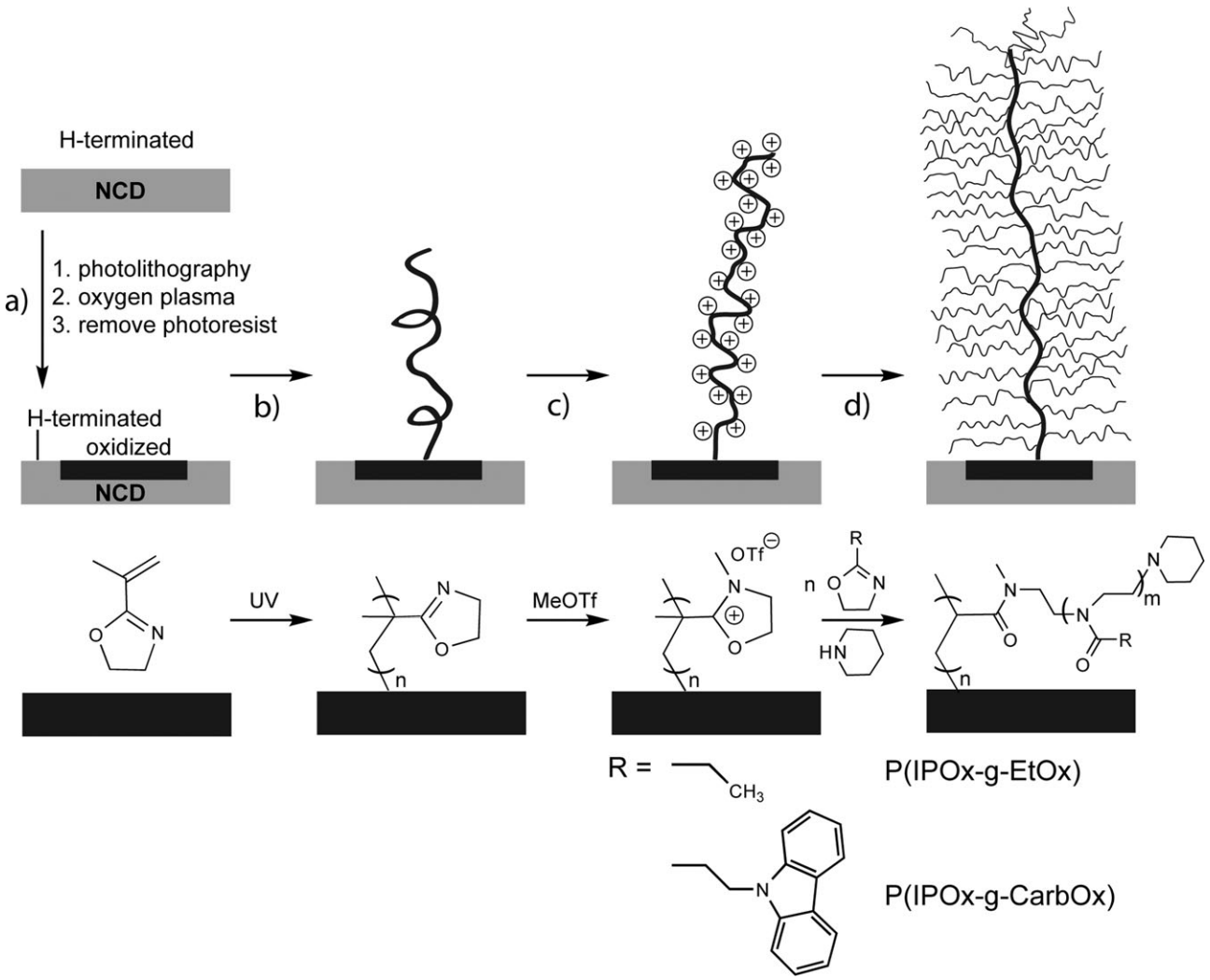

Fig. 1 Preparation of structured poly(2-oxazoline) bottle-brush brushes (BBBs) on NCD. (a) An H-terminated nanocrystalline diamond (NCD) surface was structured by photolithography and oxygen plasma. (b) PIPOx brushes were selectively formed on the oxidized NCD surface regions by UV-induced SIPGP of IPOx. (c) Conversion of the PIPOx brush backbone to the macroinitiator salt $PIPOx^{+}OTf^{-}$ by methyl triflate in acetonitrile. (d) Surface initiated LCROP of EtOx or CarbOx from the $PIPOx^{+}OTf^{-}$ macroinitiator salt and termination of the side chain polymerization with piperidine. The reaction scheme (below) outlines the surface and side chain grafting reactions resulting in dense bottle-brush brushes (BBBs).

characterized by FT-IR (Fig. 3). The strong C–F stretching mode at 1268 cm^{-1} as well as a S=O stretching band at 1025 cm^{-1} of the triflate counterion are clearly visible, proving the formation of the P($IPOx^{+}OTf^{-}$) macroinitiator brush.

Successively, the side chain LCROP was performed with the P($IPOx^{+}OTf^{-}$) macroinitiator brush and EtOx and CarbOx as the monomer to obtain BBBs. It is noteworthy that for the LCROP, the monomer was directly added to the reaction mixture without taking out the macroinitiator substrate (as for the above described IR characterization) to avoid side reactions of the reactive oxazolinium moieties. The LCROP of EtOx and CarbOx was performed overnight at 80 °C. After completion of the LCROP grafting, piperidine was added to selectively terminate the side chain polymerization. The substrate was again intensively cleaned by ultrasonication in different solvents to ensure that only chemically grafted polymer remains on the substrate before further analysis.

FT-IR spectroscopy confirmed the successful conversion of PIPOx brushes into P(IPOx-*g*-EtOx) and P(IPOx-*g*-CarbOx), respectively. The C=N (1650 cm^{-1}) and C–O (1106 cm^{-1}) stretching bands, for the pendant 2-oxazoline ring disappear and the typical characteristic amide I band for poly(2-substituted-2-oxazoline)s at 1627 cm^{-1} for P(IPOx-*g*-EtOx) and 1623 cm^{-1} for P(IPOx-*g*-CarbOx) as well as the strong CH_x deformation mode around 1450 cm^{-1} appears.[48] Additionally, the intensity increase of the aliphatic C–H stretching band between 2850 and 3000 cm^{-1} resulting in the characteristic aliphatic absorption pattern for a POx backbone indicates the formation of POx side chains in the BBs. The IR spectrum of P(IPOx-*g*-CarbOx) also exhibits an absorption band at 3041 cm^{-1} corresponding to the aromatic C–H stretching bands.

The transformation of the PIPOx brushes into BBBs was further investigated by atomic force microscopy (AFM). AFM measurements revealed a significant increase of the polymer

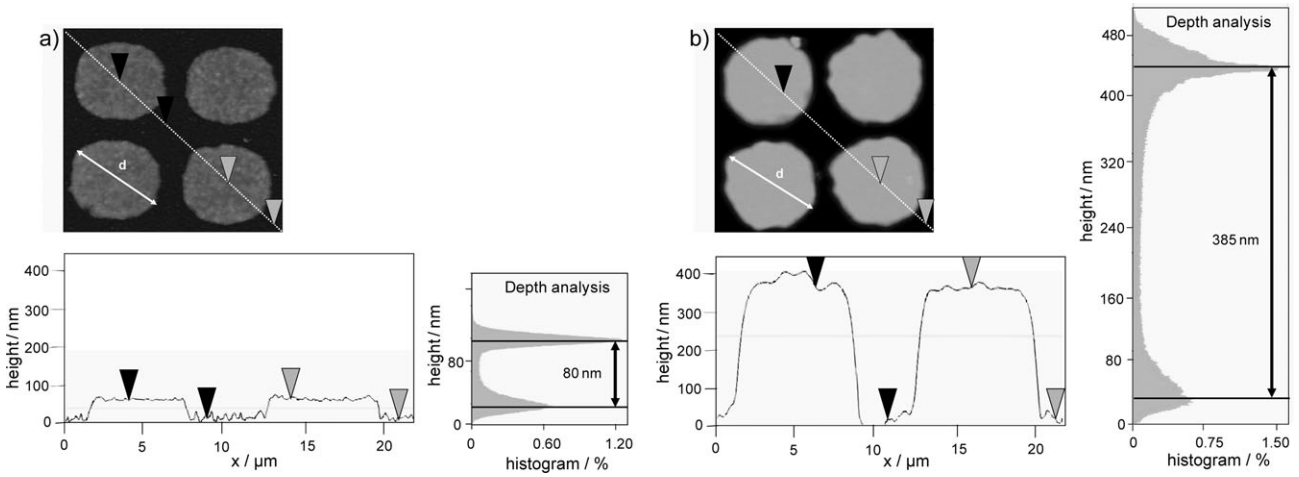

Fig. 2 AFM600 dpi) or amend the caption accordingly.?> scans (20 × 20 µm^2), section analysis and depth analysis of the patterned polymer brush structures on NCD. (a) The SIPGP of IPOx for 20 h (λ_{max} = 350 nm) results in 79 ± 8 nm thick PIPOx brushes selectively on the OH-terminated NCD regions. The native NCD regions have a roughness of 9.6 nm rms, the PIPOx coated regions of 5.4 nm rms. (b) The side chain LCROP using EtOx and termination with piperidine results in 385 ± 40 nm thick P(IPOx-*g*-EtOx) BBBs.

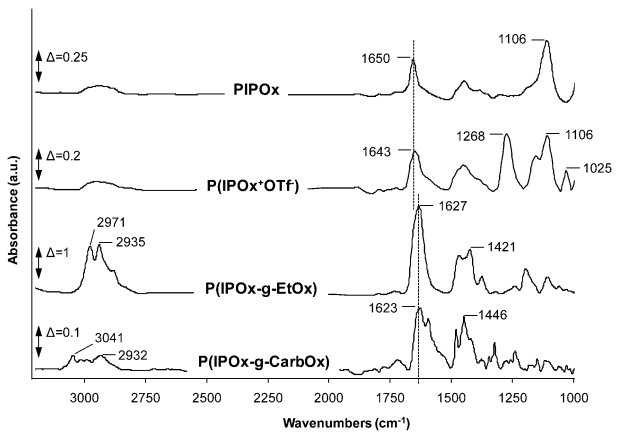

Fig. 3 FT-IR spectra of PIPOx, P(IPOx$^+$OTf$^-$) brushes as well as P(IPOx-*g*-EtOx) and P(IPOx-*g*-CarbOx) BBBs on NCD.

brush thickness. For the side chain LCROP of EtOx, the average structure height was increased from 79 ± 8 nm for the PIPOx brush to 385 ± 40 nm for the P(IPOx-*g*-EtOx) BBBs. This is consistent with our findings for the BBBs formation on glassy carbon and can be explained by the strong stretching of the bottle-brush backbone by side chain crowding.[40] The almost fivefold increase in brush thickness indicates a very high if not quantitative conversion of the pendant 2-oxazoline ring to BBBs. Furthermore, AFM measurements show an increase of the lateral structure width of around 0.5 mm. The widening of nano- and microstructured polymer brushes has been the subject of theoretical and experimental studies.[49,50] The widening is caused by the extension of grafted chains toward polymer-free surface regions and is proportional to the polymer chain molecular weight.

The conversion of PIPOx into P(IPOx-*g*-CarbOx) was also monitored by AFM. 56 ± 10 nm thick PIPOx brushes resulted in 110 ± 15 nm thick P(IPOx-*g*-CarbOx) BBB structures after the side chain LCROP of CarbOx. These experiments show that under identical reaction conditions, the layer thickness increase caused by the side chain LCROP depends on the used 2-oxazoline monomer. While a thickness increase of 393% was measured for the LCROP of EtOx, the CarbOx side chain polymerization resulted in a thickness increase of 96%. This can be explained considering that the LCROP of sterically demanding 2-substituted-2-oxazolines is significantly slower as compared to EtOx or 2-methy-2-oxazoline (MeOx).[51] The difference in the LCROP kinetics was expected and is in good agreement with our previous studies on the copolymerization of 2-oxazoline with different 2-substitutions.[52–56] However, the successful conversion of the PIPOx brush into P(IPOx-*g*-CarbOx) BBBs demonstrates that even sterically demanding 2-oxazazoline monomers can be incorporated in dense BBBs.

Polymers containing carbazole side chains are known to exhibit hole conduction. In this respect, P(IPOx-*g*-CarbOx) BBBs containing carbazole moieties are intriguing candidates for the preparation of conductive, hydrophilic and biocompatible polymer layers for amperometric biosensing. Conductivity measurements of P(IPOx-*g*-CarbOx) layers and the functionalization of such BBBs with redox proteins will be the subject of future experiments.

Besides the electron donor properties, carbazole groups are fluorescent. This allows the direct assessment of the area selective grafting reaction of P(IPOx-*g*-CarbOx) BBB structures by fluorescence microscopy. The fluorescent microscopy image taken of the BBBs of P(IPOx-*g*-CarbOx) (Fig. 4) shows a strong and selective fluorescence only at the polymer modified and initially oxidized NCD areas. No fluorescence could be observed on H-terminated NCD areas. This experiment further confirms the selective grafting of PIPOx onto the oxidized NCD areas and the successful side chain grafting of the CarbOx by LCROP. Furthermore, while we demonstrated recently that sterically demanding fluorescent dyes can be attached covalently to the BBB side chain ends, we show here that bulky fluorophores can also be introduced within the BBB side chain by means of side chain grafting.

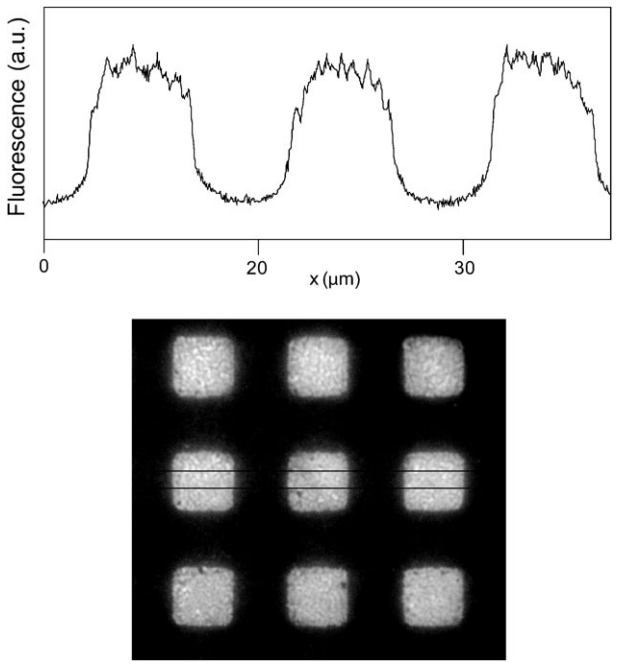

Fig. 4 Fluorescence image and average section analysis at the indicated area of a structured NCD surface, functionalized with P(IPOx-*g*-CarbOx) BBBs. The bright regions correspond to the regions of oxidized surface areas. Fluorescence was only found on the regions modified with the polymer brush.

Conclusion

Stable and homogenous microstructured PIPOx brushes were obtained by the self-initiated photografting and photopolymerization (SIPGP) of IPOx directly onto oxidized NCD. The pendant 2-oxazoline functionalities were successively converted into reactive initiator species for the side chain living cationic ring-opening polymerization (LCROP) of 2-ethyl-2-oxazoline (EtOx) as well as 2-(carbazolyl)ethyl-2-oxazoline (CarbOx). The highly reactive macroinitiator intermediate P(IPOx$^+$OTf$^-$) brushes could be isolated and were characterized by FT-IR measurements. The formation of bottle-brush brushes (BBBs) from EtOx as well as from the sterically demanding CarbOx monomer resulted in a significant increase of the polymer layer thickness indicating a strong stretching of the PIPOx backbone because of high side chain crowding. FT-IR spectroscopy and fluorescence microscopy confirmed the area selective consecutive grafting reactions. The poly(2-oxazoline) based SIPGP–LCROP approach gives access to the design of complex polymer brush architectures on diamond electrodes that allows the incorporation of a broad variety of chemical functionalities. Poly(2-oxazoline) BBBs containing hole conducting carbazole moieties on NCD are intriguing candidates for the development of biocompatible sensor systems.

Acknowledgements

This work was supported by the IGSSE ('International Graduate School for Science and Engineering') at the Technische Universität München and by the Elitenetzwerk Bayern in the frame of the international graduate school CompInt ("Materials Science of Complex Interfaces"). M.S. is additionally thankful for a postdoc fellowship from the Wacker-Institute for Silicon Chemistry at the TU München.

References

1 D. M. Gruen, *Annu. Rev. Mater. Sci.*, 1999, **29**, 211.
2 G. M. Swain, A. B. Anderson and J. C. Angus, *MRS Bull.*, 1998, **23**, 56.
3 K. Bakowicz-Mitura, G. Bartosz and S. Mitura, *Surf. Coat. Technol.*, 2007, **201**, 6131.
4 M. C. Shen, L. Martinson, M. S. Wagner, D. G. Castner, B. D. Ratner and T. A. Horbett, *J. Biomater. Sci., Polym. Ed.*, 2002, **13**, 367.
5 S. Q. Lud, M. Steenackers, R. Jordan, P. Bruno, D. M. Gruen, P. Feulner, J. A. Garrido and M. Stutzmann, *J. Am. Chem. Soc.*, 2006, **128**, 16884.
6 T. Strother, T. Knickerbocker, J. N. J. Russell, J. E. Butler, L. M. Smith and R. J. Hamers, *Langmuir*, 2002, **18**, 968.
7 B. M. Nichols, J. E. Butler, J. N. J. Russel and R. J. Hamers, *J. Phys. Chem. B*, 2005, **109**, 20938.
8 A. Hartl, E. Schmich, J. A. Garrido, J. Hernando, S. C. R. Catharino, S. Walter, P. Feulner, A. Kromka, D. Steinmuller and M. Stutzmann, *Nat. Mater.*, 2004, **3**, 736.
9 J. Rubio-Retama, J. Hernando, B. Lopez-Ruiz, A. Hartl, D. Steinmüller, M. Stutzmann, E. Lopez-Cabarcos and J. A. Garrido, *Langmuir*, 2006, **22**, 5837.
10 C. Padeste, P. Farquet, C. Potzner and H. H. Solak, *J. Biomater. Sci., Polym. Ed.*, 2006, **17**, 1285.
11 Y. Moskovitz and S. Srebnik, *Biophys. J.*, 2005, **89**, 22.
12 R. Dong, S. Krishnan, B. A. Baird, M. Lindau and C. K. Ober, *Biomacromolecules*, 2007, **8**, 3082.
13 S. P. Cullen, X. Liu, I. C. Mandel, F. J. Himpsel and P. Gopalan, *Langmuir*, 2008, **24**, 913.
14 S. P. Cullen, I. C. Mandel and P. Gopalan, *Langmuir*, 2008, **24**, 13701.
15 M. Schaeferling, S. Schiller, H. Paul, M. Kruschina, P. Pavlickova, M. Meerkamp, C. Giammasi and D. Kambhampati, *Electrophoresis*, 2002, **23**, 3097.
16 T. Matrab, M. M. Chehimi, J. O. Boudou, F. Bendic, J. Wang, N. N. Naguib and J. A. Carlisle, *Diamond Relat. Mater.*, 2006, **15**, 639.
17 L. Li, J. L. Davidson and C. M. Lukehart, *Carbon*, 2006, **44**, 2308.
18 P. Actis, M. Manesse, C. Nunes-Kirchner, G. Wittstock, Y. Coffinier, R. Boukherroub and S. Szunerits, *Phys. Chem. Chem. Phys.*, 2006, **8**, 4924.
19 M. Steenackers, S. Q. Lud, M. Niedermeier, P. Bruno, D. M. Gruen, P. Feulner, M. Stutzmann, J. A. Garrido and R. Jordan, *J. Am. Chem. Soc.*, 2007, **129**, 15655.
20 M. Steenackers, M. Jordan, A. Küller and M. Grunze, *Adv. Mater.*, 2009, **21**, 2921.
21 M. Steenackers, A. Küller, S. Stoycheva, M. Grunze and R. Jordan, *Langmuir*, 2009, **25**, 2225.
22 P. Caliceti and F. M. Veronese, *Adv. Drug Delivery Rev.*, 2003, **55**, 1261.
23 R. Duncan, *Nat. Rev. Cancer*, 2006, **6**, 688.
24 S. Zalipsky, C. B. Hansen, J. M. Oaks and T. M. Allen, *J. Pharm. Sci.*, 1996, **85**, 133.
25 Y. H. Choe, C. D. Conover, D. C. Wu, M. Royzen, Y. Gervacio, V. Borowski, M. Mehlig and R. B. Greenwald, *J. Controlled Release*, 2002, **79**, 55.
26 D. W. Branch, B. C. Wheeler, G. J. Brewer and D. E. Leckband, *Biomaterials*, 2001, **22**, 1035.
27 A. Roosjen, J. de Vries, H. C. van der Mei, W. Norde and H. J. Busscher, *J. Biomed. Mater. Res., Part B*, 2005, **73**, 347.
28 N. Adams and U. S. Schubert, *Adv. Drug Delivery Rev.*, 2007, **59**, 1504.
29 A. Mero, G. Pasut, L. D. Via, M. W. M. Fijten, U. S. Schubert, R. Hoogenboom and F. M. Veronese, *J. Controlled Release*, 2008, **125**, 87.
30 R. Konradi, B. Pidhatika, A. Mühlebach and M. Textor, *Langmuir*, 2008, **24**, 613.

31 F. C. Gaertner, R. Luxenhofer, B. Blechert, R. Jordan and M. Essler, *J. Controlled Release*, 2007, **119**, 291.
32 H. V. William, D. M. Rapti, S. Anuradha, K. Guneet, S. Gurudas and S. R. Judy, *Biotechnol. Bioeng.*, 1992, **39**, 1024.
33 A. M. Ansari, P. V. Scaria, C. Martin and M. C. Woodle, PCT, *WO* 03/066 069, 2003.
34 T. G. Bassiri, A. Levy and M. Litt, *J. Polym. Sci., Part B: Polym. Lett.*, 1967, **5**, 871.
35 T. Kagiya, S. Narisawa, T. Maeda and K. Fukui, *J. Polym. Sci., Part B: Polym. Lett.*, 1966, **4**, 441.
36 W. Seeliger, E. Aufderha, W. Diepers, R. Feinauer, R. Nehring, W. Thier and H. Hellmann, *Angew. Chem., Int. Ed. Engl.*, 1966, **5**, 875.
37 S. Huber, N. Hutter and R. Jordan, *Colloid Polym. Sci.*, 2008, **286**, 1653.
38 S. Huber and R. Jordan, *Colloid Polym. Sci.*, 2008, **286**, 395.
39 S. Cesana, J. Auernheimer, R. Jordan, H. Kessler and O. Nuyken, *Macromol. Chem. Phys.*, 2006, **207**, 183.
40 N. Zhang, M. Steenackers, R. Luxenhofer and R. Jordan, *Macromolecules*, 2009, **42**, 5345.
41 N. B. Holland, Y. X. Qiu, M. Ruegsegger and R. E. Marchant, *Nature*, 1998, **392**, 799.
42 R. A. Dwek, *Chem. Rev.*, 1996, **96**, 683.
43 X. Z. Jiang, R. A. Register, K. A. Killeen, M. E. Thompson, F. Pschenitzka and J. C. Sturm, *Chem. Mater.*, 2000, **12**, 2542.
44 N. Leclerc, A. Michaud, K. Sirois, J. F. Morin and M. Leclerc, *Adv. Funct. Mater.*, 2006, **16**, 1694.
45 B. R. Hsieh and M. H. Litt, *Macromolecules*, 1986, **19**, 516.
46 D. Petrini and K. Larsson, *J. Phys. Chem. C*, 2007, **111**, 795.
47 N. Zhang, S. Huber, A. Schulz, R. Luxenhofer and R. Jordan, *Macromolecules*, 2009, **42**, 2215.
48 R. Jordan, K. Martin, H. J. Räder and K. K. Unger, *Macromolecules*, 2001, **34**, 8858.
49 W. K. Lee, M. Patra, P. Linse and S. Zauscher, *Small*, 2007, **3**, 63.
50 M. Steenackers, A. Küller, N. Ballav, M. Zharnikov, M. Grunze and R. Jordan, *Small*, 2007, **3**, 1764.
51 K. Kempe, M. Lobert, R. Hoogenboom and U. S. Schubert, *J. Polym. Sci., Part A: Polym. Chem.*, 2009, **47**, 3829.
52 C. Taubmann, R. Luxenhofer, S. Cesana and R. Jordan, *Macromol. Biosci.*, 2005, **5**, 603.
53 K. Lüdtke, R. Jordan, P. Hommes, O. Nuyken and C. A. Naumann, *Macromol. Biosci.*, 2005, **5**, 384.
54 R. Luxenhofer and R. Jordan, *Macromolecules*, 2006, **39**, 3509.
55 S. Cesana, J. Auernheimer, R. Jordan, H. Kessler and O. Nuyken, *Macromol. Chem. Phys.*, 2006, **207**, 183.
56 T. B. Bonné, K. Lüdtke, R. Jordan and C. M. Papadakis, *Macromol. Chem. Phys.*, 2007, **208**, 1402.
57 O. A. Williams, O. Douhéret, M. Daenen, K. Haenen, E. Osawa and M. Takahashi, *Chem. Phys. Lett.*, 2007, **445**, 255.

